

Brief paper

Fault detection for nonlinear systems with uncertain parameters based on the interval fuzzy model

Simon Oblak*, Igor Škrjanc, Sašo Blažič

Faculty of Electrical Engineering, Tržaška 25, 1000 Ljubljana, Slovenia

Received 24 June 2005; received in revised form 1 August 2006; accepted 2 August 2006

Available online 2 October 2006

Abstract

In the paper an application of the interval fuzzy model (INFUMO) in fault detection for nonlinear systems with uncertain interval-type parameters is presented. A confidence band for the input–output data, obtained in the normal operating conditions of a system, is approximated using a fuzzy model with interval parameters. The approximation is based on linear programming using l_∞ -norm as a measure of the modelling error. Applying low-pass filtering when obtaining the confidence band makes it possible to use arbitrary sets of identification input signals. An application of the INFUMO in a fault-detection system for a two-tank system is presented to demonstrate the benefits of the proposed method.

© 2006 Elsevier Ltd. All rights reserved.

Keywords: Fuzzy model; Interval model; Fault detection; Interval-type uncertainties

1. Introduction

Automated supervision and fault diagnosis are important features in design of efficient and reliable production systems. Fault detection (FD) problem for linear systems has been extensively studied over the past three decades, and a lot of powerful methods have been developed. For a more thorough review, the reader is referred to survey papers by Frank (1990), Isermann (1997), and Patton and Chen (1997). However, the use of linear approaches is limited if the system to be monitored is strongly nonlinear. Since many industrial systems are nonlinear in nature, the development of nonlinear FD methods plays a significant role in practical applications. Recently, observer-based approaches (Bastin and Gevers, 1988; Chen et al., 1996; Hammouri et al., 1999), adaptive-residual-threshold approach (Frank and Ding, 1997), fuzzy-model-based (Ballé and Fuessel, 2000; Amann et al., 2001) and neural-network-based methods (Vemuri and Polycarpou, 2004; Klančar et al., 2002) have been proposed. For more information on the use of artificial intelligence in fault

detection the reader is referred to survey papers by Alcorta García and Frank (1997), Patton and Chen (1996), and Frank and Köppen-Seliger (1997). Most of the above-mentioned methods are based on a *decoupling* framework, where the modelling uncertainty and all possible faults can be decoupled through an appropriate coordinate transformation and residual generation technique. However, the modelling uncertainty is often unstructured, which makes it difficult to achieve exact decoupling between faults and modelling errors. In addition, some problems taking into consideration the input–output representation of systems as well as the design of the corresponding nonlinear observers are still open.

This paper presents a fault-detection scheme for nonlinear input–output systems with unstructured interval-type uncertainties. A fault-detection method using nonlinear adaptive fault estimators for dealing with the same system type was presented by Zhang et al. (2001). The presented approach is based on the use of an interval fuzzy model (INFUMO). Interval arithmetics has often been used in system identification, see e.g. the work by Jaulin and Walter (1993) and Malan et al. (1997), and fuzzy systems are usually applied as a nonlinear function estimators (Ying and Chen, 1997). As was introduced

*Corresponding author. Tel.: +38614768278; fax: +38614264631.

E-mail address: Simon.Oblak@fe.uni-lj.si (S. Oblak).

and shown by Škrjanc et al. (2005a), by applying only one Takagi–Sugeno-type (Takagi and Sugeno, 1985) fuzzy model with interval parameters, one is able to approximate the upper and lower boundaries of the domain of functions that result from an uncertain system. When system parameters vary in a certain tolerance band, it is advantageous to define a confidence band over a finite set of input and output measurements in which the effects of unknown process inputs are already included. If the outer bounds of the set, obtained during fault-free operating conditions, are determined, one is able to use them as the bounds of the admissible output area, and thus being able to create a simple and intuitive fault-detection system. The main idea of the proposed approach is to use the INFUMO as an admissible-filtered-output estimator in a fault-detection system. By calculating the normalized distance of the filtered system output from the boundary model outputs, a residual function is obtained.

The paper is organized in the following way. In Section 2 the system description, the main idea of interval fuzzy model identification using l_∞ -norm, the residual formation with a fault-diagnostic scenario, and detectability issues are described. Section 3 presents the two-tank system with interval-type uncertain parameters, and the application to fault detection with data pre-processing and low-pass filtering is introduced. In the final part, some outlines of future work are given.

2. Using the fuzzy interval model in fault detection

2.1. System description

Let the nonlinear system be given in a general form as follows:

$$\begin{aligned}\dot{x}(t) &= \sigma(x, u, t) + \eta(x, u, t) + \phi(x, u, t), \\ y(t) &= \gamma(x, u, t) + \rho(x, u, t),\end{aligned}\quad (1)$$

where $x \in \mathbb{R}^n$ is the state vector of the system, $u \in \mathbb{R}$ is the system input, $y \in \mathbb{R}$ denotes the system output, $\eta: \mathbb{R}^n \times \mathbb{R} \times \mathbb{R}^+ \rightarrow \mathbb{R}^n$ is the state disturbance, $\rho: \mathbb{R}^n \times \mathbb{R} \times \mathbb{R}^+ \rightarrow \mathbb{R}$ is the output disturbance, $\phi: \mathbb{R}^n \times \mathbb{R} \times \mathbb{R}^+ \rightarrow \mathbb{R}^n$ denotes the fault function, and $\sigma: \mathbb{R}^n \times \mathbb{R} \times \mathbb{R}^+ \rightarrow \mathbb{R}^n$ and $\gamma: \mathbb{R}^n \times \mathbb{R} \times \mathbb{R}^+ \rightarrow \mathbb{R}$ are the nonlinear functions of the state vector, input and time, respectively. Let us assume that only the system outputs can be directly measured. Throughout the paper the following assumptions will be made:

Assumption 1. The modelling uncertainties, represented by η and ρ in (1), are unstructured unknown nonlinear functions of x , u and t , but bounded by some known functionals (Zhang et al., 2001), i.e.,

$$\begin{aligned}|\eta(x, u, t)| &\leq \bar{\eta}(y, u, t), \quad |\rho(x, u, t)| \leq \bar{\rho}(y, u, t) \\ \forall (x, y, u) &\in \mathcal{X} \times \mathcal{Y} \times \mathcal{U}, \quad \forall t \geq 0,\end{aligned}\quad (2)$$

where the bounding functions $\bar{\eta}(y, u, t)$ and $\bar{\rho}(y, u, t)$ are known and uniformly bounded. $\mathcal{X} \subset \mathbb{R}^n$ is some compact domain of interest, and $\mathcal{U} \subset \mathbb{R}$ and $\mathcal{Y} \subset \mathbb{R}$ are the compact sets of admissible inputs and outputs, respectively.

Note that $\bar{\eta}$ and $\bar{\rho}$ are the functions of the output y whereas η and ρ are the functions of the state vector x . This is due to the fact that the states are not directly measured.

Assumption 2. The output functions $y(t)$, when $\phi(x, u, t) = 0$, are bounded by the following interval:

$$y(t) \in [\underline{y}(t), \bar{y}(t)] \subset \mathcal{Y}. \quad (3)$$

Assumption 1 characterizes the possible modelling uncertainties as unstructured but bounded by some constant or function, and Assumption 2 guarantees that in the absence of faults the bounds of the interval can be determined. As a consequence, a confidence band of outputs guarantees that a process output exhibiting normal behaviour is found in the interval $[\underline{y}, \bar{y}]$. However, due to the unknown effect of the actual disturbance functions the exact bounds cannot be defined analytically. In the paper by Fagarasan et al. (2004) two approaches to determine the boundary functions have been proposed: empirical and numerical. In the former approach, physical knowledge of the uncertainties is used to adjust its values in the model. The latter approach consists of using a constrained linear optimization technique to minimize the model precision objective function $J = (1/N) \sum_{i=1}^N (\bar{y}_i - \underline{y}_i)$, where \bar{y}_i and \underline{y}_i are the maximal and minimal output values that result from different uncertainty values. The proposed approach, introducing the interval fuzzy model, is qualitatively different because the boundary responses will be obtained by a fuzzy function approximation of the bounds of a set of filtered input–output data that already comprises the effects of disturbances.

As was shown by Ding et al. (1994) and Frank and Ding (1997), a residual generator can be designed by

$$r(t) = Q(p)(y(t) - \hat{y}(t)), \quad (4)$$

with $\hat{y}(t)$ as a process-output estimation and $Q(p)$ is a filter which enhances the residual robustness to unknown process inputs and is to be designed according to the demands of the application. Since in this case only the input and output data are available and the transfer functions from the faults and disturbances are not known, the above-mentioned approach is altered accordingly. The main idea of the presented approach is to filter both the input and output data through a low-pass filter in order to get a static input–output mapping approximation. Since the main role of the filter is to cut out the high-frequency spectre of the data set, the design procedure is further simplified by using a first-order filter. The data pairs $u_f(i)$ and $y_f(i)$, obtained in the normal operating conditions, i.e., in the absence of faults, are gathered in a set of the so-called admissible input–output data. Robustness to the effects of disturbances can be seen in the fact that the latter

are already included in the set. If the set bounds are modelled as a function of the system input, they can be used online for residual formation

$$\begin{aligned} r_{f1}(t) &= \bar{y}_f(t) - Q(p)y(t) = \bar{f}(u_f, t) - Q(p)y(t), \\ r_{f2}(t) &= Q(p)y(t) - \underline{y}_f(t) = Q(p)y(t) - \underline{f}(u_f, t), \end{aligned} \quad (5)$$

where

$$Q(p) = \frac{1}{T_f p + 1} \quad (6)$$

and T_f denotes the time constant of the filter $Q(p)$. Filtering both the input and output signals before calculation of the residuals further decreases the residual sensitivity to false alarms, resulting from the disturbances.

2.2. Interval fuzzy model

The interval fuzzy model was introduced by Škrjanc et al. (2005a) as a means of robust system identification, and it was also used in the work by Škrjanc et al. (2005b) to provide a functional description of a static nonlinear area approximation.

In this paper the modelling of $\bar{f}(u_f, t)$ and $\underline{f}(u_f, t)$ in (5) will be carried out using an interval fuzzy model. Note that for the confidence-band identification a set of either open-loop or closed-loop experiments in the absence of faults have to be conducted, and the online fault detection based on the obtained INFUMO can also be realized in both systems.

The procedure of obtaining the exact lower and upper bounds for the family of functions and assigning the INFUMO to them will be briefly reviewed. Let $C \subset \mathbb{R}$ be a compact set and $\mathcal{G} = \{g(z) : C \rightarrow \mathbb{R}\}$ be a class of nonlinear functions. Let us assume that there exist the exact upper bound \bar{g} and the exact lower bound \underline{g} that satisfy the following conditions for an arbitrary $\varepsilon > 0$ and for each $z \in C$:

$$\bar{g}(z) \geq \max_{g \in \mathcal{G}} g(z), \quad \exists g \in \mathcal{G} : \bar{g}(z) < g(z) + \varepsilon, \quad (7)$$

$$\underline{g}(z) \leq \min_{g \in \mathcal{G}} g(z), \quad \exists g \in \mathcal{G} : \underline{g}(z) > g(z) + \varepsilon. \quad (8)$$

Obtaining the bounds in Eqs. (7) and (8) would require an infinite amount of data; however, in this case we are limited to the finite set of measured filtered output values $Y = \{y_{f1}, y_{f2}, \dots, y_{fN}\}$ and the finite set of filtered input data $Z = \{z_1, z_2, \dots, z_N\} = \{u_{f1}, u_{f2}, \dots, u_{fN}\}$:

$$y_{fi} = g(z_i), \quad g \in \mathcal{G}, \quad z_i \in C \subset \mathbb{R}, \quad y_i \in \mathbb{R}, \quad i = 1, \dots, N. \quad (9)$$

The exact upper and lower boundary functions will be approximated by fuzzy functions, and the Stone–Weierstrass theorem (Ying and Chen, 1997) is extended to prove that there exist fuzzy systems \bar{f} and \underline{f} such that the bounds of an arbitrary nonlinear area can be approximated with

any precision, i.e.,

$$\begin{aligned} 0 &< \bar{f}(z_i) - g(z_i) < \varepsilon \quad \forall i, \\ -\varepsilon &< \underline{f}(z_i) - g(z_i) < 0 \quad \forall i. \end{aligned} \quad (10)$$

In this paper an INFUMO TS-type model in affine form with one antecedent variable will be assumed. It can be given as a set of rules

$$\begin{aligned} \mathbf{R}_j : \text{if } x_p \text{ is } A_j \text{ then } \bar{f}(z_i) &= \bar{y}_f = \bar{\theta}_j^T x_c, \quad j = 1, \dots, m, \\ \underline{f}(z_i) &= \underline{y}_f = \underline{\theta}_j^T x_c, \quad j = 1, \dots, m. \end{aligned} \quad (11)$$

The antecedent variable $x_p = u_f \in \mathbb{R}$ denotes the input or variable in premise, and variables $\bar{y}_f, \underline{y}_f \in \mathbb{R}$ are the outputs of the interval fuzzy model that provide the upper and lower boundary function. The antecedent variable is connected with m fuzzy sets A_j , and each fuzzy set A_j ($j = 1, \dots, m$) is associated with a real-valued function $\mu_{A_j}(x_p) : \mathbb{R} \rightarrow [0, 1]$, that produces a membership grade of the variable x_p with respect to the fuzzy set A_j . The consequent vector is denoted $x_c^T = [u_f \ 1] \in \mathbb{R}^2$. As the output functions are in affine form, 1 was added to the vector x_c . The system outputs are linear combinations of the consequent states, and $\bar{\theta}_j, \underline{\theta}_j \in \mathbb{R}^2$ are vectors of fuzzy parameters. The system in Eq. (11) can be described in closed form

$$\begin{aligned} \bar{y}_f &= \beta^T(x_p) \bar{\Theta} x_c, \\ \underline{y}_f &= \beta^T(x_p) \underline{\Theta} x_c, \end{aligned} \quad (12)$$

where $\bar{\Theta}^T = [\bar{\theta}_1, \dots, \bar{\theta}_m]$ and $\underline{\Theta}^T = [\underline{\theta}_1, \dots, \underline{\theta}_m]$ denote the upper and lower coefficient matrices for the complete set of rules, and $\beta^T(x_p) = [\beta_1(x_p), \dots, \beta_m(x_p)]$ is a vector of normalized membership functions with elements that indicate the degree of fulfilment of the respective rule. Functions $\beta_j(x_p)$ can be defined as

$$\beta_j(x_p) = \frac{\mu_{A_j}(x_p)}{\sum_{j=1}^m \mu_{A_j}(x_p)}, \quad j = 1, \dots, m, \quad (13)$$

if the partition of unity is assumed. Note that $\beta_j(x_p)$ and x_c are equal in both the upper and lower boundary-function calculations in (12).

The membership functions $\mu_{A_j}(x_p)$ and the fuzzy parameters in $\bar{\Theta}, \underline{\Theta}$ of the proposed INFUMO have to be determined for optimal approximation of the bounds. While the proper arrangement and shape of the membership functions will not be considered—the mentioned can be approached by different clustering methods (Babuška, 1998)—for the optimal fuzzy parameters the minimization of the maximum modelling error ε in Eq. (10) over the whole input set Z is performed. This implies the min–max optimization method, and l_∞ -norm is used as the modelling error measure, yielding

$$\begin{aligned} \min_{\underline{\Theta}} \max_{z_i \in Z} |y_i - \underline{f}(z_i)| \quad \text{s.t. } y_i - \underline{f}(z_i) &\geq 0, \\ \min_{\bar{\Theta}} \max_{z_i \in Z} |y_i - \bar{f}(z_i)| \quad \text{s.t. } y_i - \bar{f}(z_i) &\leq 0, \end{aligned} \quad (14)$$

where $\underline{f}(z_i) = \beta^T \underline{\Theta} x_c(z_i)$ and $\bar{f}(z_i) = \beta^T \bar{\Theta} x_c(z_i)$. Note that the data are obtained by sampling different functions from \mathcal{G} with arbitrary values of z_i . The solutions to both problems can be found by linear programming, because both problems can be viewed as linear programming problems. This brings simplicity to the realization of the optimizing process. However, large data sets and a large number of parameters will still pose a threat to optimization convergence. In the first case the problems are approached with data-reduction methods, and in the latter case, on the other hand, solutions to reduce the number of parameters have to be found.

2.3. Formation of the proposed fault-detection system

When the parameter identification is done, the INFUMO is connected to the process in parallel to get online estimations of the boundary outputs. In terms of fault detection, the decision function should consist of verifying that each measurement belongs to the corresponding confidence band. In order to provide normalized quantitative information about the proximity of the measurements to the closest interval bound, distances were used, as presented by Fagarasan et al. (2004). If a filtered output value $y_f(t)$ belongs to an interval $[\underline{y}_f(t), \bar{y}_f(t)]$, and if $\tilde{y}_f(t)$ denotes the mean interval value

$$\tilde{y}_f(t) = \frac{\bar{y}_f(t) + \underline{y}_f(t)}{2} \tag{15}$$

the proposed distance is defined in the following way:

$$\begin{aligned} \text{if } y_f(t) < \tilde{y}_f(t), \quad d(y_f) &= \frac{y_f(t) - \tilde{y}_f(t)}{\underline{y}_f(t) - \tilde{y}_f(t)}, \\ \text{if } y_f(t) > \tilde{y}_f(t), \quad d(y_f) &= \frac{y_f(t) - \tilde{y}_f(t)}{\bar{y}_f(t) - \tilde{y}_f(t)}. \end{aligned} \tag{16}$$

The distance in (16) is zero when the measurement is equal to \tilde{y}_f , and approaches the value 1 if the measurement is close to one of the interval bounds. A fault is signalled every time $d(y_f)$ exceeds the value 1. Fig. 1 gives a schematic representation of the proposed fault-detection system. The filter $Q(p)$ is represented by a block denoted LPF (low pass filter), and the distance is calculated in the DIST block.

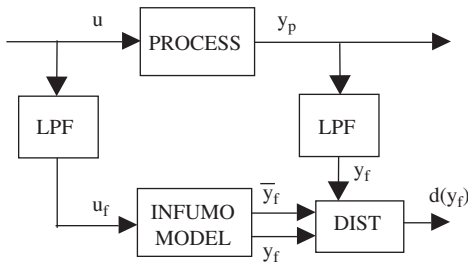


Fig. 1. Fault-detection system using static INFUMO model.

2.3.1. Detectability properties

To study the detectability properties of the proposed method the worst-case scenario will be considered. In this sense the following theorem guarantees detectability of a fault ϕ :

Theorem 1. Let the contribution of a fault $\phi(x, u, t)$ to the filtered process output be denoted $y_{\phi f}(t)$, and the difference between the boundary functions $\bar{y}_f(t) - \underline{y}_f(t) = \lambda(t)$. A fault will certainly be detected if the absolute value of the former is greater than the width of the output confidence band, i.e.

$$|y_{\phi f}(t)| > \lambda(t). \tag{17}$$

Proof. For the purpose of fault-detectability analysis, the output function in Eq. (1) will be rewritten to

$$y_f(t) = Q(p) \cdot y(t) = y_{0f}(t) + \rho_f(t) + y_{\phi f}(t), \tag{18}$$

where $y_{0f}(t)$, $\rho_f(t)$ and $y_{\phi f}(t)$ denote the filtered contributions of the “undisturbed” output, disturbances and fault, respectively. Since the upper and lower confidence-band bounds $\bar{y}_f(t)$ and $\underline{y}_f(t)$ were obtained in the experiments where no faults were present, the following inequalities hold:

$$\begin{aligned} y_{0f}(t) + \rho_f(t) - \underline{y}_f(t) &\geq 0, \\ \bar{y}_f(t) - y_{0f}(t) - \rho_f(t) &\geq 0. \end{aligned} \tag{19}$$

By adding the fault contribution $y_{\phi f}(t)$ to both sides of (19), the following can be written:

$$\begin{aligned} y_{0f}(t) + y_{\phi f}(t) + \rho_f(t) - \underline{y}_f(t) &\geq y_{\phi f}(t) \Rightarrow y_{\phi f}(t) \leq y_f(t) - \underline{y}_f(t), \\ \bar{y}_f(t) - y_{0f}(t) - \rho_f(t) - y_{\phi f}(t) &\geq -y_{\phi f}(t) \Rightarrow \bar{y}_f(t) - y_f(t) \\ &\geq -y_{\phi f}(t). \end{aligned} \tag{20}$$

Hence, $y_{\phi f}(t)$ is bounded by $y_f(t) - \bar{y}_f(t) \leq y_{\phi f}(t) \leq y_f(t) - \underline{y}_f(t)$. When no fault is detected, i.e., $\underline{y}_f(t) \leq y_f(t) \leq \bar{y}_f(t)$, inequality (20) can be further extended to

$$\begin{aligned} y_{\phi f}(t) \leq y_f(t) - \underline{y}_f(t) &= (\bar{y}_f(t) - \underline{y}_f(t)) + (y_f(t) - \bar{y}_f(t)) \\ &= \lambda(t) + (y_f(t) - \bar{y}_f(t)) \leq \lambda(t) + 0 \\ &= \lambda(t), \\ -y_{\phi f}(t) \leq \bar{y}_f(t) - y_f(t) &= (\bar{y}_f(t) - \underline{y}_f(t)) + (\underline{y}_f(t) - y_f(t)) \\ &= \lambda(t) + (\underline{y}_f(t) - y_f(t)) \leq \lambda(t) + 0 \\ &= \lambda(t). \end{aligned} \tag{21}$$

Both inequalities in (21) can be united to

$$|y_{\phi f}(t)| \leq \lambda(t). \tag{22}$$

When a fault is not detected, inequality (22) is satisfied, thus implying that in the case when $|y_{\phi f}(t)| > \lambda(t)$ the fault is certainly detected.

Remark 1. If the steady-state gain of the filter is $Q(s)|_{s=0} = 1$, and if

$$\int_{1/T}^{\infty} |Y_{\phi}(\omega)|^2 d\omega \ll \int_0^{1/T} |Y_{\phi}(\omega)|^2 d\omega \quad (23)$$

holds for any $y_{\phi}(t)$, i.e., the dominant part of spectral power density is at low frequencies with respect to the LPF bandwidth $1/T$, then $y_{\phi f}(t) \doteq y_{\phi}(t)$ and the condition in (22) can be extended to $|y_{\phi}(t)| \leq \lambda'(t)$ where $\lambda'(t) \doteq \lambda(t)$.

3. Simulation example

In this section the benefits of the proposed method will be illustrated by a simulation example. A well-known benchmark problem will be considered. It deals with a laboratory plant using two tanks with fluid flow, as was described by Zhang et al. (2004). The two cylindrical tanks are identical, with a cross section $A_s = 0.0154 \text{ m}^2$. The cross section of the connection pipe and the outlet pipe is $S_{p1} = S_{p2} = 3.6 \times 10^{-5} \text{ m}^2$, and the liquid levels in the two tanks are denoted h_1 and h_2 , respectively. The plant-setup scheme is presented in Fig. 2. The supplying flow rates coming from an electric pump to tank 1 are denoted $q_1(t)$, and there is an outflow from tank 2 denoted $q_2(t)$. Using the mass balance equations and Toricelli's rule, the following equations are obtained:

$$\begin{aligned} \dot{h}_1 &= \frac{1}{A_s} (-K_{p1} \text{sign}(h_1 - h_2) \sqrt{2g|h_1 - h_2|} + q_1), \\ \dot{h}_2 &= \frac{1}{A_s} (K_{p1} \text{sign}(h_1 - h_2) \sqrt{2g|h_1 - h_2|} - K_{p2} \sqrt{2gh_2}), \end{aligned} \quad (24)$$

where $K_{p1} = a_1 S_{p1}$ and $K_{p2} = a_2 S_{p2}$ denote the outflow constants, and g is the gravity acceleration. Let $a_1 = a_2 = 1$ for the sake of simplicity.

To get an input–output system that is similar to industrial processes the model will be modified in the following way. The input to the system is the electric-pump

voltage $u_1(t)$ that produces the inlet flow

$$\bar{q}_1(t) = K_u(1 + v_1(t))u_1(t), \quad (25)$$

where K_u is the voltage-to-flow-conversion constant, and $v_1(t)$ denotes the inaccuracy of the conversion. The only measurable output signal is the voltage of the pressure sensor, converting the fluid level $h_2(t)$ in tank 2 into the output voltage $u_2(t)$ according to the following equation:

$$u_2(t) = K_h(1 + v_2(t))h_2(t), \quad (26)$$

where K_h is the height-to-voltage-conversion constant, and $v_2(t)$ denotes the inaccuracy of the conversion. The values of the constants are $K_u = 8.8 \times 10^{-6} \text{ m}^3/\text{Vs}$ and $K_h = 16.667 \text{ V/m}$, and the upper bounds of the inaccuracies are $\bar{v}_1 = \bar{v}_2 = 0.03$.

The set of faults under consideration will follow the examples presented in Zhang et al. (2002, 2004). It will consist of the following faults:

- *Actuator fault in the pump:* A simple multiplicative actuator fault is assumed by letting the actual inlet flow be described by $q_1(t) = \bar{q}_1(t) + (1 - K_f)\bar{q}_1(t)$, where $\bar{q}_1(t)$ is the flow in the non-fault case, and $K_f \in [0, 1]$ is the fault constant.
- *Leakage in tank 1:* The leak is assumed to be circular in shape and of unknown radius r_1 . As a consequence, the outflow rate of the unknown-size leak is $q_{f1} = a_1 \pi (r_1)^2 \sqrt{2gh_1}$.
- *Leakage in tank 2:* Analogously to the case of leakage in tank 1, the outflow rate is $q_{f2} = a_2 \pi (r_2)^2 \sqrt{2gh_2}$.

With reference to the given INFUMO identification procedure, a confidence band of input–output data must be defined. This band will also include all unexpected output deviations due to parameter uncertainties. A set of 20 experiments was carried out. The inputs and associated output signals are shown in Fig. 3. For the sake of brevity, only the first, the second, and the last data sets are presented. One of the major benefits of the interval fuzzy model identification, shown in Fig. 3, is that the input signals can be arbitrary.

According to Eq. (4), the input and output signals are subjected to low-pass filtering (LPF). The structure of the LPF was chosen as a simple first-order system, represented by the transfer function in Eq. (6). The optimal design of the LPF time constant T_f was not considered in this study. The filter can also be seen as a means of trade-off between the fault-detecting speed and robustness to false alarms. The cut-off frequency ω_f was chosen according to the absolute values of the Fourier transforms of the output signals, as presented in Fig. 4. Hence, the filter time constant was defined as $T_f = 1/\omega_f = 476 \text{ s}$. The lower diagram of Fig. 4 demonstrates the absolute values of the Fourier transforms of the filtered outputs. This way a compact set of measurements that represents steady-state system behaviour is obtained. It can be seen as an approximation of a static input–output mapping area.

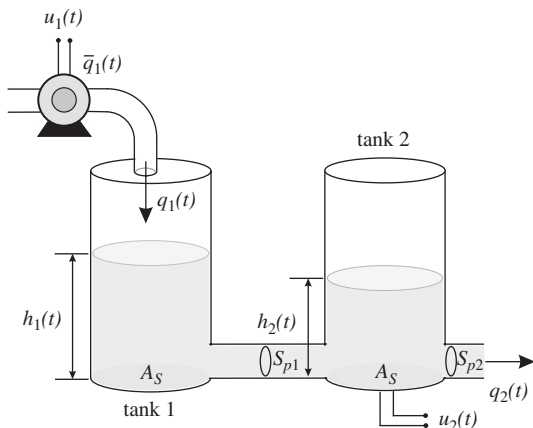


Fig. 2. Two-tank laboratory plant.

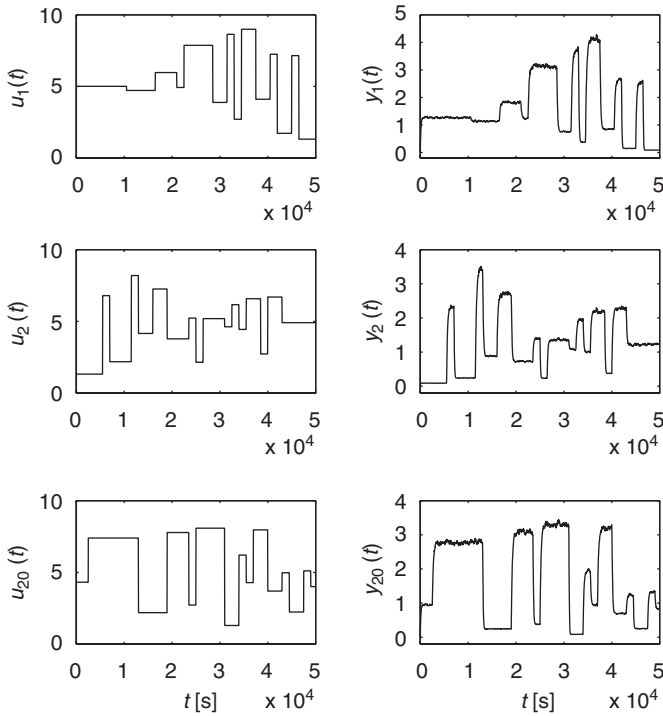


Fig. 3. Inputs and outputs: the first, the second, and the last experiment.

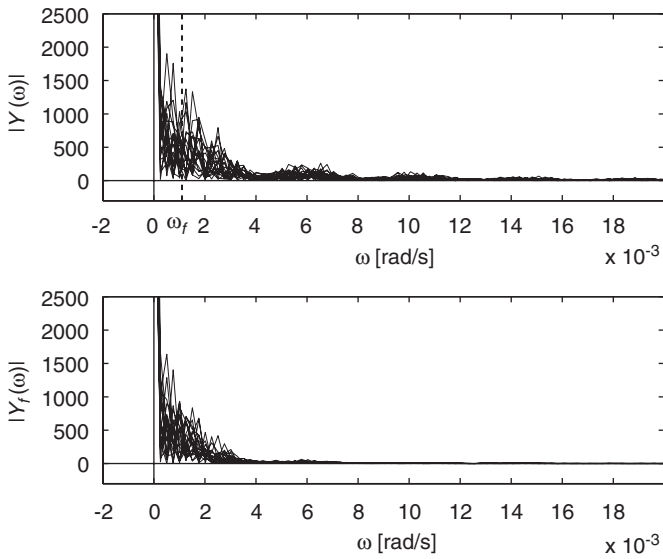


Fig. 4. The choice of the filter cut-off frequency.

The identification experiments resulted in a huge set of data. To avoid the problems with optimization convergence, data reduction is performed by determining the boundary points. Firstly, the range of input measurements is divided into equidistant subspaces. The length of the step is chosen according to the subspace with the highest density of data. In each subspace the extremal points are determined. The input–output data is presented in Fig. 5, and the resulting set of 302 boundary points is emphasized. These data were used as the training data set for the INFUMO identification. A static INFUMO can be

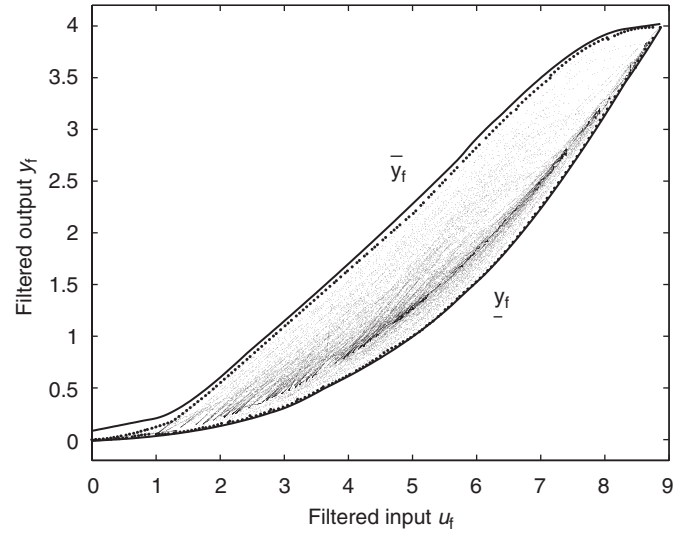


Fig. 5. Set of filtered input–output data with boundary points and boundary INFUMO functions.

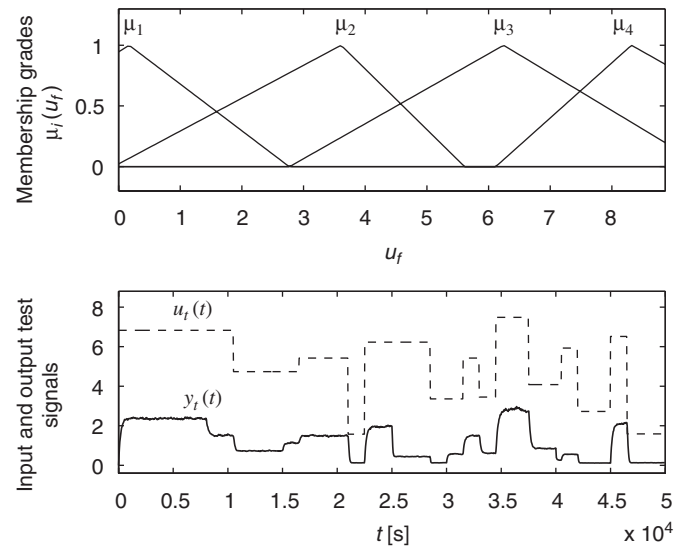


Fig. 6. Membership-function arrangement and test experiment signals.

employed. This brings additional reduction of the number of fuzzy parameters to be optimized. The membership functions of the INFUMO antecedent variables were of triangular shape and arranged using grid partitioning (Babuška, 1998). According to the data-area shape, it was sufficient to use four fuzzy subsets for the upper and lower fuzzy functions.

The parameters were optimized using the proposed INFUMO optimization algorithm in Eq. (14). The resulting boundary functions can be seen in Fig. 5. It is evident that the min–max optimization gave satisfactory results in approximating the given area.

To realize a fault-detection system, INFUMO is connected to the process in parallel, as shown in Fig. 1. In the test experiment a 20% actuator fault ($K_f = 0.2$) is assumed to occur in time period $t_{act} = 8000–15000$ s, a

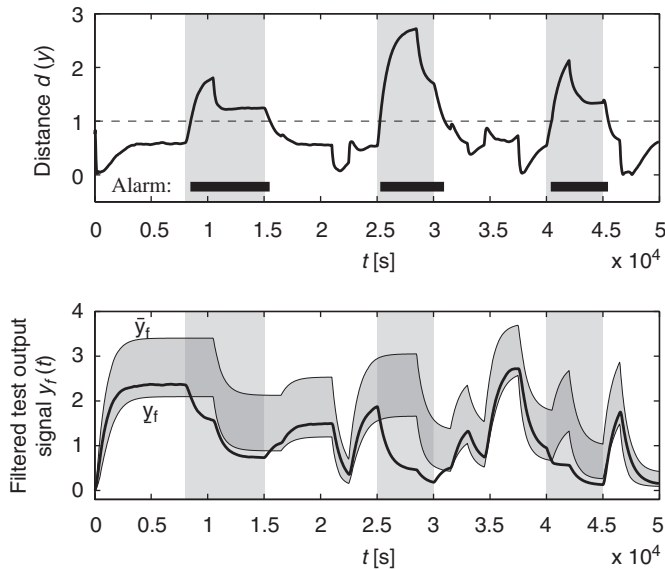


Fig. 7. Results of the fault detection system.

leakage of $r_1 = 3 \times 10^{-3}$ m in tank 1 at $t_{leak1} = 25\,000$ – $30\,000$ s, and a leakage of $r_2 = 3 \times 10^{-3}$ m in tank 2 at $t_{leak2} = 40\,000$ – $45\,000$ s, respectively. The input test signal and the corresponding process output signal are presented in the lower plot of Fig. 6. The results of the test run can be seen in Fig. 7. The first diagram demonstrates the calculation of the distance function, and in the second diagram time-dependent courses of the filtered process output y_f and the INFUMO boundary functions $\bar{y}_f, \underline{y}_f$ are shown. It is evident that the proposed FD system successfully tracks the filtered output crossing of the permitted band, denoting the expected normal system behaviour. In the shaded areas, i.e., where the faults from the fault set occurred, fault is declared with reasonably small time delays, depending on the time constant of the proposed low-pass filter: 467.7, 288.0, and 380.2 s, respectively.

4. Conclusion

A novel approach of the fault-detection system design for nonlinear input–output systems was presented. The interval fuzzy model (INFUMO), which is suitable for robust identification of nonlinear functions, was applied to the residual generation and decision stages. The benefit in fault detection is to be able to directly model a family of fault-free system responses from the confidence band, which already includes the effects of uncertainties, based only on the input–output data. Employing the low-pass filtering to obtain the input–output data set, relatively simple fuzzy functions are sufficient to provide a fairly efficient fault-detection system.

The filter served as a trade-off between the speed of the FD-system and robustness to false alarms; however, investigating the performance resulting from different choices of filter structure, the extension of the presented

INFUMO-based FD method to fault isolation, and investigating possible extensions to frequency-based methods and fault-tolerant control deserves further attention. In addition, the results of the simulated example demonstrate the quality of performance coupled with simplicity of application, which is very important from the application point of view.

Acknowledgements

This work was supported by the Ministry of Higher Education, Science and Technology of Republic of Slovenia.

References

- Alcorta García, E., Frank, P.M., 1997. Deterministic nonlinear observer-based approaches to fault diagnosis: a survey. *Control Engineering Practice* 5 (5), 663–670.
- Amann, P., Perronne, J.M., Gissinger, G.L., Frank, P.M., 2001. Identification of fuzzy relational models for fault detection. *Control Engineering Practice* 9, 555–562.
- Babuška, R., 1998. *Fuzzy Modeling for Control*. Kluwer Academic Publishers, Boston, USA.
- Ballé, P., Fuessel, D., 2000. Closed-loop fault diagnosis based on a nonlinear process model and automatic fuzzy rule generation. *Engineering Applications of Artificial Intelligence* 13 (6), 695–704.
- Bastin, G., Gevers, M.R., 1988. Stable adaptive observers for nonlinear time-varying systems. *IEEE Transactions on Automatic Control* 33, 650–658.
- Chen, J., Patton, R.J., Zhang, H.-Y., 1996. Design of unknown input observers and robust fault detection filters. *International Journal of Control* 63 (1), 85–105.
- Ding, X., Guo, L., Frank, P.M., 1994. Parameterization of linear observers and its application to observer design. *IEEE Transactions on Automatic Control* 39 (8), 1648–1652.
- Fagarasan, I., Ploix, S., Gentil, S., 2004. Causal fault detection and isolation based on a set-membership approach. *Automatica* 40, 2099–2110.
- Frank, P.M., 1990. Fault diagnosis in dynamic systems using analytical and knowledge-based redundancy—a survey and some new results. *Automatica* 26, 459–474.
- Frank, P.M., Ding, X., 1997. Survey of robust residual generation and evaluation methods in observer-based fault detection systems. *Journal of Process Control* 7 (6), 403–424.
- Frank, P.M., Köppen-Seliger, B., 1997. New developments using ai in fault diagnosis. *Engineering Applications of Artificial Intelligence* 10 (1), 3–14.
- Hammouri, H., Kinnaert, M., El Yaagoubi, E., 1999. Observer-based approach to fault detection and isolation for nonlinear systems. *IEEE Transactions on Automatic Control* 44 (10), 1879–1884.
- Isermann, R., 1997. Supervision, fault-detection and fault-diagnosis methods—an introduction. *Control Engineering Practice* 5 (5), 639–652.
- Jaulin, L., Walter, E., 1993. Set inversion via interval analysis for nonlinear bounded-error estimation. *Automatica* 29 (4), 1053–1064.
- Klančar, G., Juričić, D., Karba, R., 2002. Robust fault detection based on compensation of the modelling error. *International Journal of Systems Science* 33 (2), 97–105.
- Malan, S., Milanese, M., Taragna, M., 1997. Robust analysis and design of control systems using interval arithmetic. *Automatica* 33 (7), 1363–1372.
- Patton, R.J., Chen, J., 1996. Neural networks in fault diagnosis of nonlinear dynamic systems. *Engineering Simulation* 13 (6), 905–924.

- Patton, R.J., Chen, J., 1997. Observer-based fault detection and isolation: Robustness and applications. *Control Engineering Practice* 5 (5), 671–682.
- Škrjanc, I., Blažič, S., Agamennoni, O., 2005a. Identification of dynamical systems with a robust interval model. *Automatica* 41 (2), 327–332.
- Škrjanc, I., Blažič, S., Agamennoni, O., 2005b. Interval fuzzy modelling applied to wiener models with uncertainties. *IEEE Transactions on Systems, Man and Cybernetics, Part B: Cybernetics* 35 (5), 1092–1095.
- Takagi, T., Sugeno, M., 1985. Fuzzy identification of systems and its applications to modelling and control. *IEEE Transactions on Systems, Man, and Cybernetics* 15, 116–132.
- Vemuri, A.T., Polycarpou, M.M., 2004. A methodology for fault diagnosis in robotic systems using neural networks. *Robotica* 22, 419–438.
- Ying, H., Chen, G., 1997. Necessary conditions for some typical fuzzy systems as universal approximators. *Automatica* 33, 1333–1338.
- Zhang, X., Polycarpou, M.M., Parisini, T., 2001. Robust fault isolation for a class of non-linear input–output systems. *International Journal of Control* 74 (13), 1295–1310.
- Zhang, X., Polycarpou, M.M., Parisini, T., 2002. A robust detection and isolation scheme for abrupt and incipient faults in nonlinear systems. *IEEE Transactions on Automatic Control* 47 (4), 576–593.
- Zhang, X., Parisini, T., Polycarpou, M.M., 2004. Adaptive fault-tolerant control of nonlinear uncertain systems: An information-based diagnostic approach. *IEEE Transactions on Automatic Control* 49 (8), 1259–1274.